




ORIGINAL RESEARCH

Consistency of spatio-temporal patterns of avian migration across the Swiss lowlands

Philippe Tschanz^{1,2,3} , Loïc Pellissier^{2,3} , Xu Shi^{1,4} , Felix Liechti¹  & Baptiste Schmid¹ ¹Swiss Ornithological Institute, Sempach, Switzerland²Landscape Ecology, Institute of Terrestrial Ecosystems, Department of Environmental System Science, ETH Zurich, Zurich, Switzerland³Swiss Federal Research Institute WSL, Birmensdorf, Switzerland⁴Chair of Wildlife Ecology and Management, University of Freiburg, Freiburg, Germany

Keywords

Avian migration, flight behavior, migration intensity, prediction, radar ornithology

Correspondence

Philippe Tschanz, Swiss Ornithological Institute, Seerose 1, 6204 Sempach, Switzerland. Tel: +41 41 462 97 00; Fax: +41 462 97 10; E-mail: philippe.tschanz@protonmail.com

Editor: Ned Horning

Associate Editor: Matthew Van Den Broeke

Received: 2 October 2019; Revised: 22 November 2019; Accepted: 25 November 2019

doi: 10.1002/rse2.143

Remote Sensing in Ecology and Conservation 2020;6 (2):198–211

Abstract

Each year, billions of birds migrate across the continents by day and night through airspaces increasingly altered by human activity, resulting in the deaths of millions of birds every year through collisions with man-made structures. To reduce these negative impacts on wildlife, forecasts of high migration intensities are needed to apply mitigation actions. While existing weather radar networks offer a unique possibility to monitor and forecast bird migration at large spatial scales, forecasts at the fine spatial scale within a complex terrain, such as the mountainous Swiss landscape, require a small-scale network of ornithological radars. Before attempting to build such a network, it is crucial to first investigate the consistency of the migratory flow across space and time. In this study, we simultaneously operated three ornithological radar systems across the Swiss lowlands to assess the spatio-temporal consistency of diurnal and nocturnal bird movements during the spring and autumn migration season. The relative temporal course of migration intensities was generally consistent between sites during peak migration, in particular for nocturnal movements in autumn, but absolute intensities differed greatly between sites. Outside peak migration, bird movement patterns were much less consistent and, unexpectedly, some presumably non-migratory bird activity achieved intensities close to peak migration intensities, but without spatial correlations. Only nocturnal migration intensity in autumn could be predicted with consistently high accuracy, but including parameters of atmospheric conditions in the model improved predictability of diurnal movements considerably. Predictions for spring were less reliable, probably because we missed an important part of the migration season. Our results show that reliable forecasts of bird movements within a complex terrain call for a network of year-round bird monitoring systems, whereas accurate information of atmospheric conditions can help to limit the number of measurement points.

Introduction

Each year, billions of birds migrate between breeding and wintering grounds, playing an important role in the functioning of ecosystems and providing a multitude of services and disservices (Bauer and Hoyer 2014; Bauer et al. 2017). However, many migratory bird species are endangered, facing substantial declines (Sanderson et al. 2006; Kirby et al. 2008; Vickery et al. 2014), and with the rapid expansion of human activities into the aerosphere (e.g.

aviation, light pollution, building of tall structures such as skyscrapers, wind energy facilities, or power lines), aerial conflicts have been on the rise (Shamoun-Baranes et al. 2017). Measures to mitigate this aerial human–wildlife conflict include reducing the spatial and temporal concurrence of birds and human activities, or focusing mitigation measures during times of intense migration (Bauer et al. 2017; Shamoun-Baranes et al. 2017), such as temporary shutdown of wind turbines (Hüppop et al. 2006), altering civil or military flight plans (Shamoun-Baranes

et al. 2008), or turning off artificial lights (Van Doren et al. 2017). However, to implement such measures, we need to enhance our understanding of the spatio-temporal dynamics of migrating birds and make reliable predictions. An improved understanding of migration in space and time will also help answer many grand challenges of migration ecology, such as identification of migration routes or crucial stopover sites (Bauer et al. 2019).

Most migration occurs in a broad front that is highly dynamic in both space and time, and affected by topography and atmospheric conditions (Richardson 1990; Bruderer 2003; Nilsson et al. 2019). In autumn, migrants approaching Switzerland with southwesterly directions from a relatively wide catchment area are funneled through the Swiss lowlands, which are confined by the Jura Mountains in the northwest and the much higher Alpine massif in the south (Bruderer and Jenni 1990; Bruderer and Liechti 1990; Bruderer 2017). In spring, however, migrants approaching Switzerland with northeasterly directions are mostly deviated around Switzerland by these mountain chains (Liechti et al. 1996; Bruderer 1999). While diurnal migration is strongly concentrated within the lowest few hundreds of meters above ground level, nocturnal migration is much more distributed in height (Bruderer et al. 2018). Migrating birds select periods with favorable weather conditions, which can lead to enormous day-to-day variations in migration intensities and concentrates migration to short periods within the migration season (e.g. Erni et al. 2002; Van Belle et al. 2007; Nilsson et al. 2019). Commonly found weather variables that influence migration intensities are wind conditions, precipitation, temperature and atmospheric pressure (Richardson 1990).

Previous studies used various modeling and technological approaches to predict bird migration patterns. Local-scale radar studies showed that migration is forecastable based on atmospheric conditions (e.g. Erni et al. 2002; Van Belle et al. 2007). Recently, a model to forecast bird migration across the United States using a network of weather radars has been developed (Van Doren and Horton 2018), and a Europe-wide system is within reach (Nilsson et al. 2019; Nussbaumer et al. 2019). These systems offer the unique possibility to monitor and forecast bird migration at the continental scale, but they are not adequate to provide migration forecasts over a complex terrain, such as the mountainous Swiss landscape, because of the inadequate coverage of low flight altitudes (Hüppop et al. 2019). Instead of using radar, Liechti et al. (2013) and Aurbach et al. (2018) simulated the migrants' behavior in relation to topography and wind conditions across Switzerland. They showed the major flyways which migrants are expected to take and how they respond to obstacles ahead under

different wind conditions. These models allow providing decision makers with maps identifying potential high collision risk areas for regional planning processes, but are not suited to provide dynamic patterns of local bird concentrations and collision risks (Liechti et al. 2013). An application of measures to prevent fatal bird collisions, like temporal shutdown systems for wind turbines (Marques et al. 2014) or lights-out regimes for tall buildings (Loss et al. 2014), call for accurate forecasting of local bird concentrations both in space and time. Similar to local weather forecasts, this requires a prediction model based on a network of automated local observation points for bird movements, complemented by large-scale, continental measurements. While the European weather radar network can provide valid information on the large-scale pattern of nocturnal bird migration intensities (Metz et al. 2017; Nilsson et al. 2019), there are no comparable data available on the local scale. Before attempting to build such a network, it is crucial to investigate the consistency of the migratory flow across space and time.

The aim of this study was to investigate the consistency of the migratory flow across the whole extent of the Swiss lowlands. We simultaneously operated three ornithological radar systems, day and night, to assess the spatial and temporal consistency of bird movement activity during the spring and autumn migration seasons. We first compared the temporal course of diurnal and nocturnal bird activity between sites for spring and autumn movements. We then used measured bird movement intensities at a site to predict bird movement intensities at other radar sites. Finally, we tested whether including atmospheric conditions or restricting the data to peak migration periods improved prediction outcomes.

Materials and Methods

Study area and period

In 2017, three BirdScan MR1 ornithological radar systems were operated across the Swiss lowlands. The radars were located in southwestern (Geneva: 46°10'N, 05°59'E, 401 m above sea level [a.s.l.]), central (Sempach: 47°07'N, 08°11'E, 516 m a.s.l.), and northeastern (Winterthur: 47°29'N, 08°43'E, 462 m a.s.l.) Switzerland and continuously operated from 30 March to 13 June, and from 7 August to 29 October. The sites were roughly aligned along the main seasonal direction of migration as indicated by the distribution of flight directions (Fig. 1). The Swiss lowlands lie between 400 and 700 m a.s.l. and are delimited topographically to the northwest by the Jura Mountains with elevations up to 1720 m a.s.l., and to the south by the Alps with many mountain peaks exceeding

4000 m a.s.l. Both mountain ranges extend in an arc from the northeast to the southwest (Fig. 1).

Radar data

The BirdScan MR1 is a recently developed radar system for the continuous and real-time monitoring of bird movement activity (Swiss BirdRadar Solution AG, www.swiss-birdradar.com). It uses a vertically directed cone-shaped beam (25 kW pulsed X-band) and operated in short pulse mode (65 ns, range resolution 7.5 m) within 50 to 1500 m above ground level (a.g.l.). Maximum detection range, however, depends on the size of the object and is at about 800 m a.g.l. for small passerines (Schmid et al. 2019). The rotating antenna is inclined by 2° from the vertical axis, resulting in a nutating movement that tracks objects within the radar beam and allows for objects flying close to the center of the radar beam to derive its flight direction and ground speed. The antenna rotated for half of the measurement period, and remained static otherwise, that is, echoes were registered without information on flight speed and direction. Based on characteristics of the echo signatures, the BirdScan classifies echoes as bird or non-bird (insect or non-biological scatterer), and further classifies bird echoes into different bird

types (Zaugg et al. 2008). Additional technical details on the BirdScan are given in Schmid et al. (2019); field validation of the BirdScan with other radar systems are given in Nilsson et al. (2018) and Liechti et al. (2019).

Only echoes classified as bird were used. Nocturnal bird movements for a day were defined from civil dusk of that day to civil dawn of the following day, and diurnal bird movements from civil dawn to civil dusk of the same day. We computed daily/nightly mean values of the flight directions, concentrations of flight directions (hereafter directional concentrations) and bird traffic rates (BTRs). Flight directions and directional concentrations were computed using the subset of echoes that contained directional information. Directional concentration was estimated using the length of the resultant mean direction vector r , which ranges from 0 (randomly distributed) to 1 (perfectly aligned) (Batschelet 1981). BTR is the number of birds crossing a virtual transect of 1 km length perpendicular to the flight direction within an hour. Its definition is identical to the commonly used migration traffic rate (MTR; Lowery 1951; Bruderer 1971) but includes both migratory and non-migratory movements. We accounted for distance-dependent variation in surveyed volume and for size-class specific detection probability of the radar system by weighing each echo with its estimated

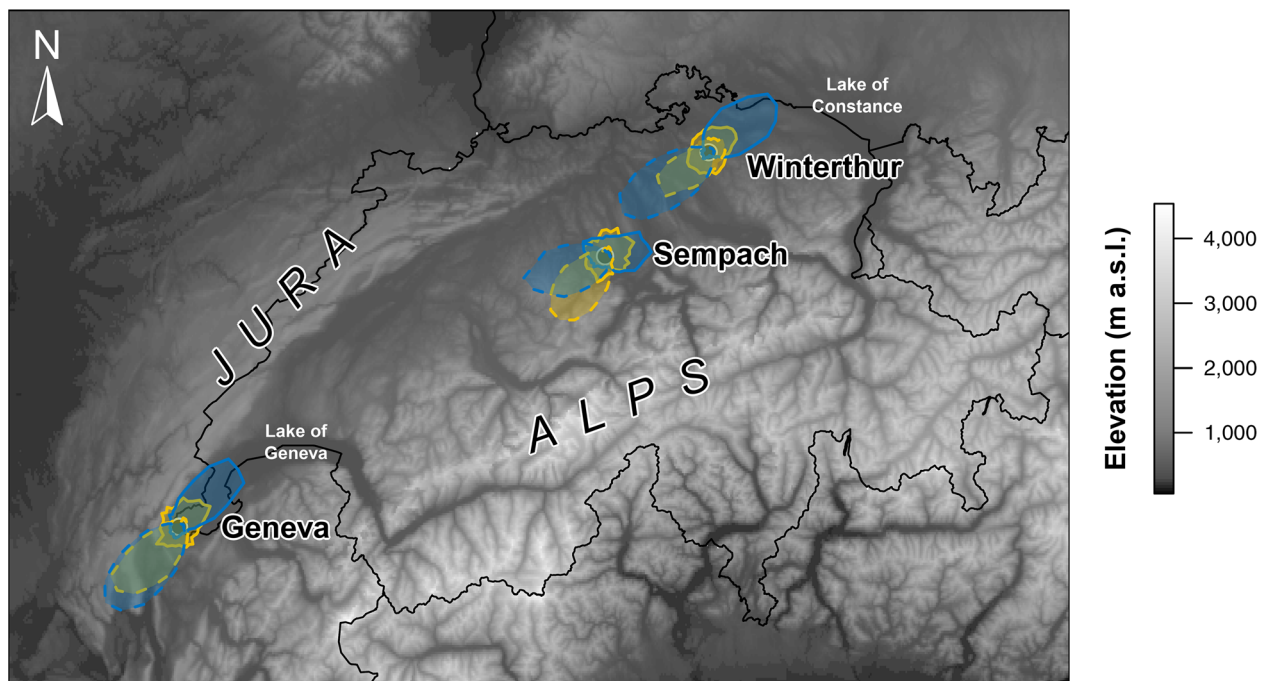


Figure 1. Topographical map of Switzerland with the distribution of flight directions at the study sites. The polygons show the relative distribution of flight directions for all bird movements within the study duration for nocturnal (blue) and diurnal (yellow) activity in spring (solid lines) and autumn (dashed lines) within 50 to 1500 m a.g.l. [data sources: country boundaries (GADM 2018); digital elevation model (Jarvis et al. 2008)].

correction factor (Schmid et al. 2019). Strong precipitation, technical problems, and switching between protocols caused some radar blind times. When radar blind times exceeded 80% of a day/night, we did not validate the BTR estimates but still used the detected echoes to calculate the directional concentration. Because the radar system did not distinguish between the different sources of the blind time, we tended to overestimate BTRs in days/nights with precipitation events, and therefore to underestimate the effects of rain on BTRs. This is because bird activity is likely reduced during radar blind times caused by strong precipitation compared to radar operating times, whereas bird activity likely remains similar during both radar operating times and technical radar blind times. In addition, to avoid echo miss-classification, we manually excluded echoes registered during periods with precipitation.

Atmospheric data

Precipitation data were retrieved from meteorological field stations operated by the Federal Office of Meteorology and Climatology (MeteoSwiss, www.meteoswiss.admin.ch) closest to the respective radar site: Aadorf-Tänikon (47°29'N, 08°54'E, 13 km east from radar in Winterthur), Geneva-Cointrin (46°15'N, 06°08'E, 14 km northeast from radar in Geneva), and Lucerne (47°02'N, 08°18'E, 13 km southeast from radar in Sempach). Wind, atmospheric pressure, and air temperature data were extracted from the COSMO-1 model at the respective radar location as hourly values between 50 and 1500 m a.g.l. every 50 m. The COSMO-1 is a version of the COSMO (Consortium for small-scale modeling, www.cosmo-model.org) family of numerical weather prediction models with a grid box size of 1.1 km and is operated by MeteoSwiss.

Atmospheric data were processed to get daily/nightly averages per site according to civil twilight. Wind profit was calculated as the daily/nightly average wind profit from the first up to the third quartile of the distribution of flight altitudes for the respective day/night. For days/nights with less than 15 echoes, wind profit was averaged over 50–1500 m a.g.l. We defined wind profit as the length of the wind vector along the preferred seasonal flight direction, using the formula:

$$WP = v_{\text{wind}} \cos(\alpha_{\text{wind}} - \alpha_{\text{bird}}),$$

where wind profit (WP, m s^{-1}) equaled wind speed (v_{wind} , m s^{-1}) times the cosine of the angle between the direction the wind was blowing to (α_{wind}) and the preferred seasonal flight direction (α_{bird}), which was estimated as the overall mean flight direction per season and

site. Thus, we used a α_{bird} of 30° (Geneva), 58° (Sempach), and 44° (Winterthur) in spring, and 223° (Geneva), 242° (Sempach), and 233° (Winterthur) in autumn. Wind profit was used as a general measure of how supportive wind conditions were per day/night. We did not consider different bird drift strategies or flight behavior and assumed that wind blowing in the direction of the mean flight direction is beneficial (Kemp et al. 2012). For precipitation, we used the precipitation duration data and expressed it as the daily/nightly proportion of time with precipitation. For temperature and pressure, we used their hourly values extracted at 50 m a.g.l. and computed their 24 h changes as additional variables.

Spatio-temporal patterns of bird movements

We explored the spatio-temporal patterns of bird movements by comparing the temporal course of BTRs between sites, separately for diurnal/nocturnal and spring/autumn movements. We defined the main migration periods for each of these movement categories to explore whether bird activity patterns were more consistent within peak migration periods than outside, and to test whether restricting our data to the main migration periods improved predictions (see below).

The main migration period was defined based on the temporal course of the directional concentration. We presumed that high directional concentrations are connected to migratory movements, while low directional concentrations are caused by local movements. We estimated temporal trends of the directional concentration for each site separately and an overall trend using weighted local polynomial regression. The main migration period was then defined as the time period from the inflection point left to the inflection point right of the maxima of the overall trend of the directional concentration (Fig. 2). When no inflection point was found because the observation period started too late or ended too early, the start or end time of the observation period was used to delineate the main migration period. Because the trend was always low for diurnal spring movements (Fig. 2A), we considered the whole observation period to belong to local movements and excluded it for the analysis restricted to the main migration period. Consequently, our migration periods were defined from 30 March to 17 May (spring, night), from 22 September to 29 October (autumn, day), and from 7 August to 29 October (autumn, night).

Predicting bird movement intensities

To assess the spatio-temporal consistency of bird movement intensities across the Swiss lowlands, we fitted

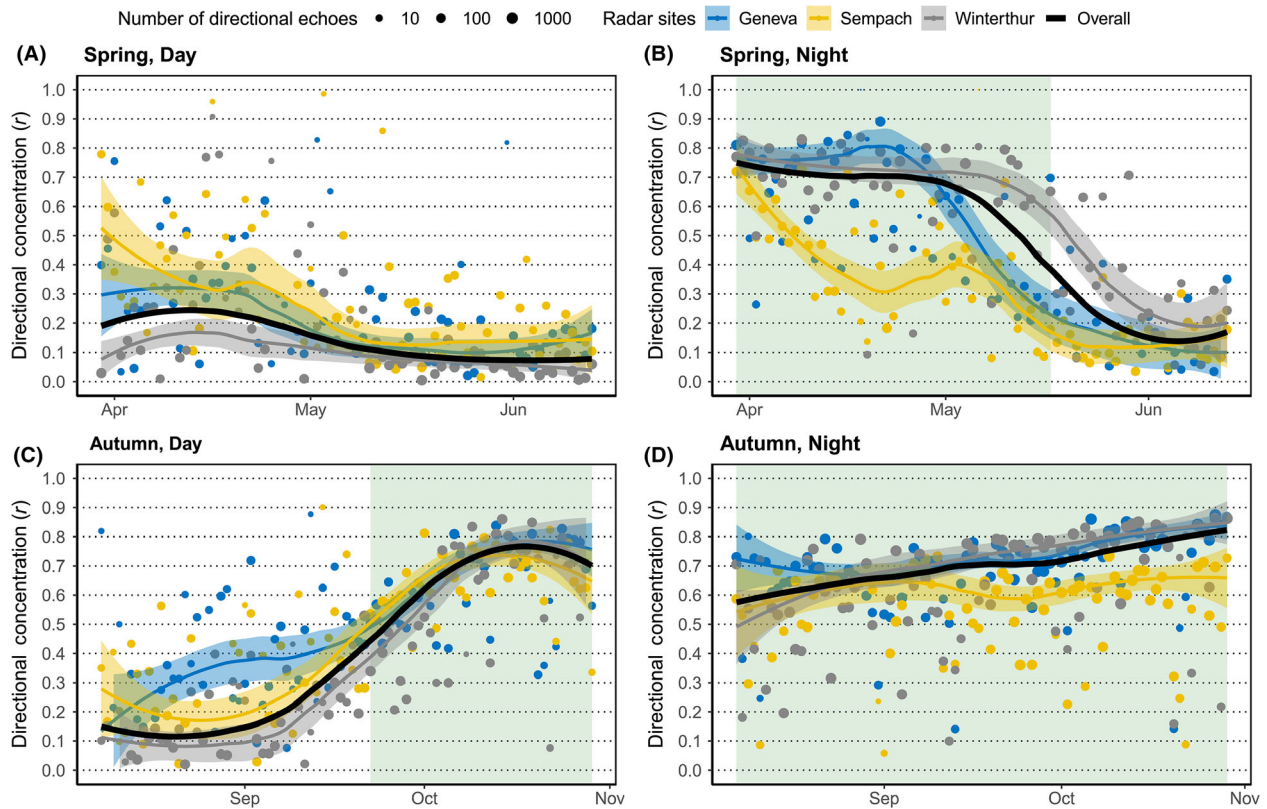


Figure 2. Seasonal course of the directional concentration r (length of the resultant mean flight direction vector) for (A) diurnal spring, (B) nocturnal spring, (C) diurnal autumn, and (D) nocturnal autumn bird movements. Dots indicate the daily mean r for the three sites: Geneva (blue), Sempach (yellow), and Winterthur (grey). The area of the dot is proportional to the logarithm of the number of directional echoes. Curves indicate the temporal trend of r at the different sites. The thick black curve shows the overall temporal trend for all sites combined. The green background indicates the time period that was defined as the main migration period. The trend was estimated using weighted local polynomial regression.

regression models using a site's observed BTR to predict another site's BTR for the same day/night (hereafter BTR models). Furthermore, we fitted regression models that additionally included atmospheric conditions at the prediction site and differences in atmospheric conditions between the prediction and explanatory site (hereafter BTR + Atmo models) to test if including atmospheric conditions improves predictability. Both model types were fitted separately for (1) each pairwise combination between the three sites, (2) diurnal and nocturnal movements, and (3) spring and autumn movements. In total, this resulted in 24 model combinations per model type. We ran this analysis twice, once using data from the full observation period, and once with data restricted to the main migration period to test whether spatio-temporal patterns of bird movements were more consistent during peak migration.

Regression models were fitted in R version 3.6.0 (R Core Team 2019) using generalized linear models with gamma distribution and log-link function. A gamma

distribution was used, since BTR is a continuous variable (count data standardized in time and space), strictly positive and the gamma distribution additionally estimates a dispersion parameter (Faraway 2006). BTR models used another site's BTR (BTR_x) as only predictor variable. BTR + Atmo models additionally included the following atmospheric predictor variables: wind profit differences between sites ($\Delta_{xy}WP$) precipitation duration (proportional to the length of the respective day/night) differences between sites ($\Delta_{xy}PD$), atmospheric pressure at the prediction site (P_y), 24 h change in atmospheric pressure at the prediction site $\Delta_{24h}P_y$, air temperature at the prediction site (T_y), 24 h change in air temperature at the prediction site ($\Delta_{24h}T_y$) (see Table S1 for further details). We used differences in atmospheric conditions between sites for wind profit and precipitation because they can be highly variable on a local scale and because we expected these differences to at least partly explain between-sites differences in BTRs. For temperature and pressure, however, we used their local manifestation at

the prediction site, as these variables were highly correlated between sites (Fig. S1). We log-transformed BTR_x and standardized all atmospheric predictors (mean = 0, standard deviation = 1) to allow comparison of their relative effects instead of a variable selection approach. The standardized atmospheric estimates with their corresponding 95% confidence intervals were then used to investigate the effects of the different atmospheric variables on BTR.

We checked for potential multicollinearity problems of the predictor variables using the variance inflation factor (VIF). VIF was below 4 for all predictor variables in all models, thus, multicollinearity was no problem (Zuur et al. 2007; Sheather 2009). We also checked for temporal autocorrelation of the residuals by inspecting the autocorrelation function. Many of the BTR models showed clear signs of temporal autocorrelation, but including the atmospheric predictors largely removed temporal autocorrelation in all but five models. Since our goal was to assess the predictability of BTR using only data from the same day without relying on past information that may not be available, we refrained from time series analysis. Despite temporal autocorrelation, we used all models for the assessment of the prediction performance. However, to assess the effects of the atmospheric variables, we used only the 43 (out of 48) BTR + Atmo models with no or negligible temporal autocorrelation.

Model prediction performance was assessed using the mean Spearman's rank correlation coefficient ρ between the observed and the predicted BTRs obtained from 10-fold cross-validation. Spearman's rank correlation was used because variables were non-normally distributed. First, we split the data randomly into ten sets of similar size and then fitted the model to 90% of the data and predicted the remaining left-out 10% of the data. This was repeated ten times until all left-out data was predicted. We then computed the Spearman's ρ between the observed and the predicted data. Finally, we repeated these steps ten times and used the mean Spearman's ρ to compare predictive performances between seasons, time of day, and model types.

Results

Spatio-temporal patterns of bird movements

The temporal course of both diurnal and nocturnal BTR was relatively similar between Geneva and Sempach in both seasons, but there were major differences with respect to diurnal migration in Winterthur from May to August (Fig. 3). BTRs were higher in autumn compared

to spring, and higher for nocturnal compared to diurnal activity (Table 1).

In spring, diurnal BTRs remained low (<300 birds $\text{km}^{-1} \text{h}^{-1}$) in Geneva and Sempach in April, but slowly increased in May up to about 900 birds $\text{km}^{-1} \text{h}^{-1}$ around mid-May, before slowly decreasing to relatively constant levels around 300 birds $\text{km}^{-1} \text{h}^{-1}$ (Fig. 3A top). Distinct from the other sites, diurnal BTRs in Winterthur increased continuously from the beginning of May until mid-June and reached the highest BTRs in June with nearly 2500 birds $\text{km}^{-1} \text{h}^{-1}$. On most days, BTR in Winterthur was much higher compared to the other sites, sometimes more than one order of magnitude. At night, BTRs in Sempach and Geneva varied around the seasonal mean BTR of about 400 birds $\text{km}^{-1} \text{h}^{-1}$ and showed only a mild trend of higher BTRs in April and June (Fig. 3A bottom). Winterthur showed a similar pattern, but with much higher peaks (up to 3300 birds $\text{km}^{-1} \text{h}^{-1}$) than at the other sites during April.

In autumn, diurnal BTRs were mostly below 500 birds $\text{km}^{-1} \text{h}^{-1}$ in Geneva and Sempach until mid-September when they quickly increased and reached highest intensities at the end of September (Geneva: ~ 1200 birds $\text{km}^{-1} \text{h}^{-1}$) or in mid-October (Sempach: ~ 1000 birds $\text{km}^{-1} \text{h}^{-1}$) (Fig. 3B top). In Winterthur, the highest diurnal BTRs were reached already at the beginning of August (~ 2100 birds $\text{km}^{-1} \text{h}^{-1}$) and continuously decreased until mid-September. From the end of September, BTRs in Winterthur varied around levels similar to the other sites. At night, the temporal course of BTRs was relatively similar at all sites with an increase in activity from mid-September to mid-October, where the highest BTRs occurred (Geneva: ~ 7200 birds $\text{km}^{-1} \text{h}^{-1}$, Sempach: ~ 5200 birds $\text{km}^{-1} \text{h}^{-1}$, Winterthur: ~ 9100 birds $\text{km}^{-1} \text{h}^{-1}$) (Fig. 3B bottom).

Predicting bird movement intensities

Prediction accuracy of BTR models differed markedly between seasons and time of day (Fig. 4, Table S2). For spring movements, predictions for diurnal activity (mean Spearman's $\rho \pm$ standard deviation = 0.51 ± 0.17) were more accurate on average than for nocturnal activity ($\rho = 0.36 \pm 0.11$; Fig. 4A). Restricting the data to the main migration period somewhat improved BTR models for nocturnal activity ($\rho = 0.49 \pm 0.08$; Fig. 4C). For autumn movements, nocturnal activities were predicted with consistently high accuracy ($\rho = 0.79 \pm 0.01$), whereas predictions for diurnal activity were poor on average ($\rho = 0.24 \pm 0.44$) but ranged from $\rho = -0.44$ to 0.70 (Fig. 4B). Restricting the data to the main migration period, however, improved predictions for diurnal autumn activity considerably ($\rho = 0.65 \pm 0.09$; Fig. 4D).

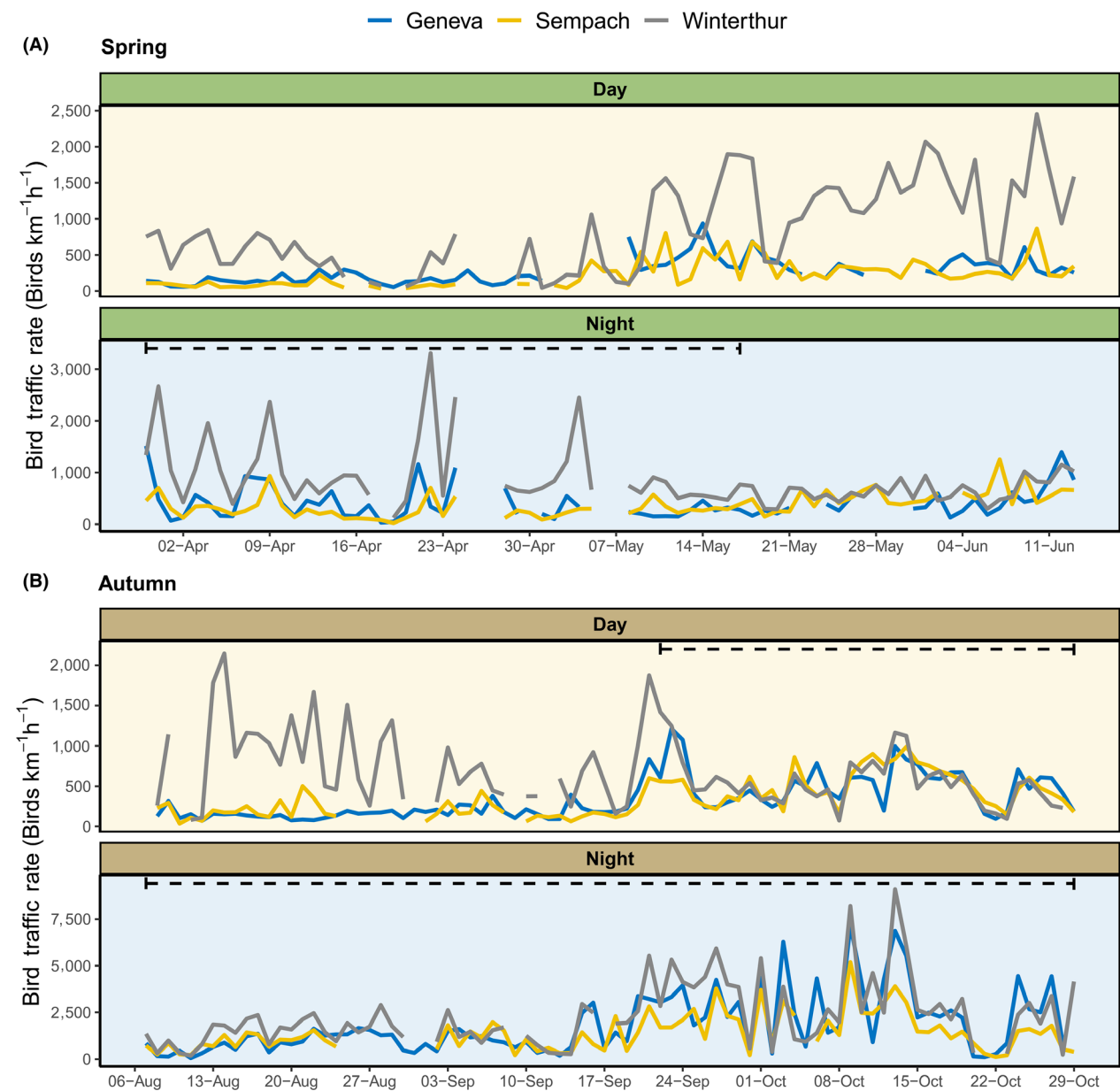


Figure 3. Seasonal course of daily mean bird traffic rates (BTRs) in (A) spring and (B) autumn for diurnal (yellowish background) and nocturnal (bluish background) activity at the three radar sites: Geneva (blue lines), Sempach (yellow lines), and Winterthur (grey lines). The horizontal black dashed lines delineate the main migration period as defined based on the temporal course of the concentration of flight directions (see Materials & methods and Fig. 2 for details).

No consistent relationship of prediction accuracy and distance between explanatory and predictor site was observed using the data for the full period (Fig. 4A and B). When restricting the data to the main migration period, predictions between the closest sites mostly performed best (Fig. 4C and D). This was consistent with closer sites showing higher correlations of observed BTRs for data restricted to the main migration

period (Fig. S3), but not when using the full data (Fig. S2).

Including atmospheric conditions generally improved predictions, but to different extents depending on the season, time of day, and time period of data used (Fig. 4, Table S2). For spring, models with atmospheric parameters (BTR + Atmo) performed better than models without atmospheric parameters (BTR) for both diurnal

Table 1. Means, standard deviations (SD), and sample sizes (*N*) of daily/nightly bird traffic rates (BTRs) and directional concentrations *r* per season, time of day (ToD), and site for the full and main migration period

Season	ToD	Site	Full period				Migration period			
			BTR		<i>r</i>		BTR		<i>r</i>	
			Mean (SD)	<i>N</i>	Mean (SD)	<i>N</i>	Mean (SD)	<i>N</i>	Mean (SD)	<i>N</i>
Spring	Day	Geneva	271 (174)	67	0.25 (0.19)	70	-	-	-	-
		Sempach	229 (189)	69	0.29 (0.23)	71	-	-	-	-
		Winterthur	880 (602)	70	0.18 (0.20)	72	-	-	-	-
	Night	Geneva	406 (320)	64	0.45 (0.27)	66	387 (332)	43	0.58 (0.21)	45
		Sempach	379 (234)	70	0.32 (0.22)	71	285 (181)	44	0.43 (0.21)	45
		Winterthur	860 (591)	71	0.51 (0.25)	73	991 (701)	44	0.65 (0.18)	46
Autumn	Day	Geneva	337 (255)	83	0.49 (0.22)	83	510 (259)	38	0.63 (0.15)	38
		Sempach	352 (240)	75	0.49 (0.22)	78	505 (226)	38	0.65 (0.11)	38
		Winterthur	675 (444)	77	0.37 (0.27)	82	554 (307)	37	0.57 (0.21)	37
	Night	Geneva	1826 (1616)	83	0.68 (0.14)	84	1826 (1616)	83	0.68 (0.14)	84
		Sempach	1395 (1009)	76	0.54 (0.16)	79	1395 (1009)	76	0.54 (0.16)	79
		Winterthur	2316 (1772)	78	0.63 (0.19)	83	2316 (1772)	78	0.63 (0.19)	83

Missing values are indicated by '-'.

(BTR + Atmo: $\rho = 0.66 \pm 0.15$; BTR: $\rho = 0.51 \pm 0.17$) and nocturnal movements (BTR + Atmo: $\rho = 0.57 \pm 0.17$; BTR: $\rho = 0.36 \pm 0.11$) (Fig. 4A). For autumn, models with atmospheric parameters performed similar for nocturnal movements (BTR + Atmo: $\rho = 0.82 \pm 0.03$; BTR: $\rho = 0.79 \pm 0.01$), but much better for diurnal movements (BTR + Atmo: $\rho = 0.66 \pm 0.13$; BTR: $\rho = 0.24 \pm 0.44$) than models without atmospheric parameters (Fig. 4B). Restricting the data to the main migration periods, models for nocturnal activity performed somewhat better with atmospheric parameters than without, but not for diurnal movements (Fig. 4C and D, Table S2).

Wind, precipitation, pressure, and temperature clearly influenced BTRs. Effect sizes of the atmospheric predictor variables (i.e. the standardized regression coefficients) showed a similar pattern both for models that use the whole observation period and for those that use only the main migration period (Fig. 5A and B). Effect sizes were mostly positive for wind profit ($\Delta_{xy}WP$), except for diurnal activity in spring (where they were mostly negative), and mostly negative for precipitation duration ($\Delta_{xy}PD$). Effect sizes of pressure (P_y) tended to be negative in spring and positive in autumn, whereas effect sizes of temperature (T_y) were mostly positive in spring and during the day in autumn, but mostly negative at night in autumn. Between-site difference in pressure ($\Delta_{24h}P_y$) and temperature ($\Delta_{24h}T_y$) had mostly small effect sizes with 95% confidence intervals encompassing zero.

Discussion

Our study has shown that the relative temporal course of bird activity patterns across the Swiss lowlands is

relatively consistent during peak migration, in particular for nocturnal movements in autumn, but that absolute intensities can differ greatly between locations. Outside peak migration periods, bird activity patterns were much less consistent, and some presumably non-migratory bird activity achieved intensities close to peak migration intensities. Including atmospheric conditions improved predictability of bird movement intensities considerably. A major drawback was the late start of the joint measurement campaign in spring, which missed a relevant period of migratory movements.

The inconsistent spatio-temporal patterns of bird activity outside the peak migration periods (Fig. 3) with low directional concentrations (Fig. 2) are probably the result of non-migratory activity, such as foraging and dispersal flights. Likely, these non-migratory movements are mainly dominated by local factors, and hardly correlated between the three sites. Hence, we assume that the high intensity of non-migratory diurnal movements from mid-May to mid-June (Fig. 3A) and in August (Fig. 3B) above Winterthur are governed by aerial feeders, mainly by Common Swifts (*Apus apus*). They are known to arrive/leave around these times and breed in large colonies in the vicinity of the radar site within the city (Weitnauer 1980; Winkler 1999). The other two sites are situated in the countryside, where aerial feeders are present but much less concentrated. Such local factors probably also explain why activity patterns were not consistently more similar between close sites (cf. Sempach and Winterthur) than between sites further apart (cf. Sempach and Geneva) (Fig. 4A and B, Fig. S2). These local factors, however, appeared to become less relevant during peak migration, since restricting the data to the main migration periods

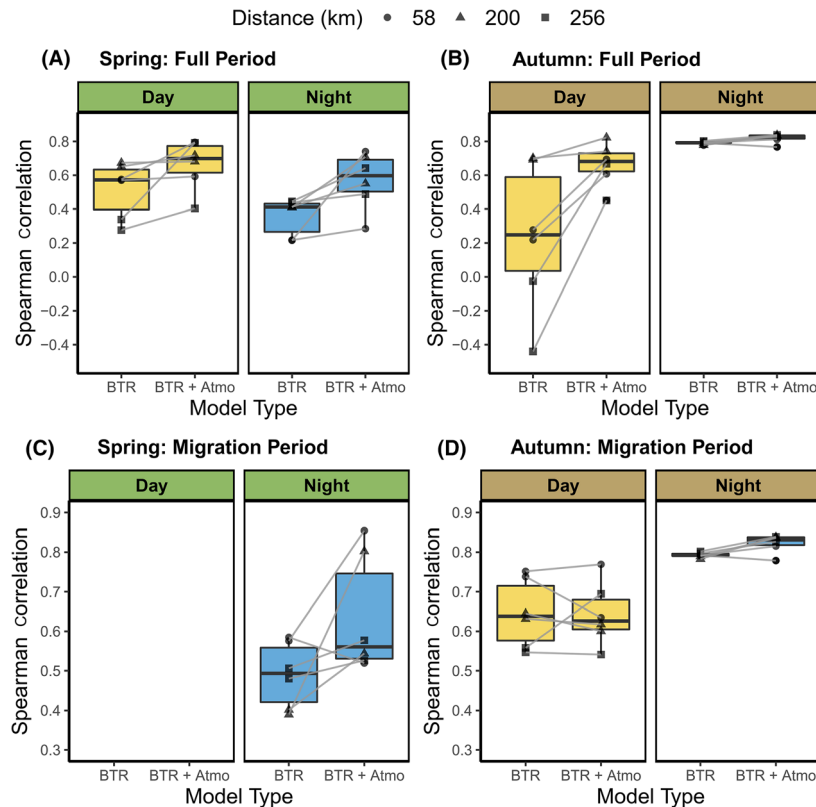


Figure 4. Comparison of prediction performance for diurnal (yellow boxes) and nocturnal (blue boxes) bird movements in (A) spring and (B) autumn during the full time period, respectively in (C) spring and (D) autumn restricted to the main migration period (note the different scale of the y-axis). 'BTR' models used BTR from another site as only predictor variable, whereas 'BTR + Atmo' models additionally included atmospheric conditions. The symbols show the mean Spearman correlation between observed and predicted BTR for the respective model type, season, time of day, and combination between the site used as predictor and the site where predictions were made. The shape of the symbols indicates the distance between the explanatory and prediction site. The grey lines connect the mean Spearman correlation of the 'BTR' and 'BTR + Atmo' models using the same combination of explanatory and prediction site to illustrate the effect of atmospheric conditions on prediction performance. Boxplots summarize the prediction performance of the six models. Boxes range from the first to the third quartile, horizontal bars indicate the median, and the whiskers extend to the last observation within 1.5 times the interquartile range from the box. No results are shown for diurnal spring bird movements in (C) because the main migration period was missed.

reduced the between-sites variation in prediction accuracy and closer sites tended to produce better predictions (Fig. 4C and D, Fig. S3).

The higher consistency of nocturnal compared to diurnal activity during peak migration (Figs. 3 and 4) may be related to the generally different composition and strategy of birds predominantly migrating by day or night. Soaring species that depend on thermals, and swallows, that mix migration with hunting flights, primarily migrate during the day (Bruderer 2003, 2017; Newton 2008). Otherwise diurnal migration is dominated by short-distance migrants that use more of a 'fly-and-forage' strategy (Strandberg and Alerstam 2007): they restrict their migratory bouts to a few hours per day, generally in the morning. In addition, they generally fly at lower altitudes (Bruderer et al. 2018) and hence follow the terrain more

strongly than nocturnal migrants. Nocturnal migratory birds, on the other hand, fly during longer flight stages and at higher altitudes, and are therefore less influenced by the terrain underneath them (Bruderer 2003, 2017; Newton 2008). With an average ground speed of 12 m s^{-1} (Bruderer 1997), a passerine can cover the distance between Winterthur and Geneva (256 km) in only 6 h. It may well be that a nocturnal migrant passes both sites within a single night, whereas a diurnal migrant with a 'fly-and-forage' strategy may stopover in between. Therefore, the distances between monitoring sites, from the viewpoint of flight time, is shorter in nocturnal than diurnal migration. Consequently, spatial correlations for nocturnal migration is rather compact in time, whereas spatial correlations for diurnal migration are likely spaced out over several days.

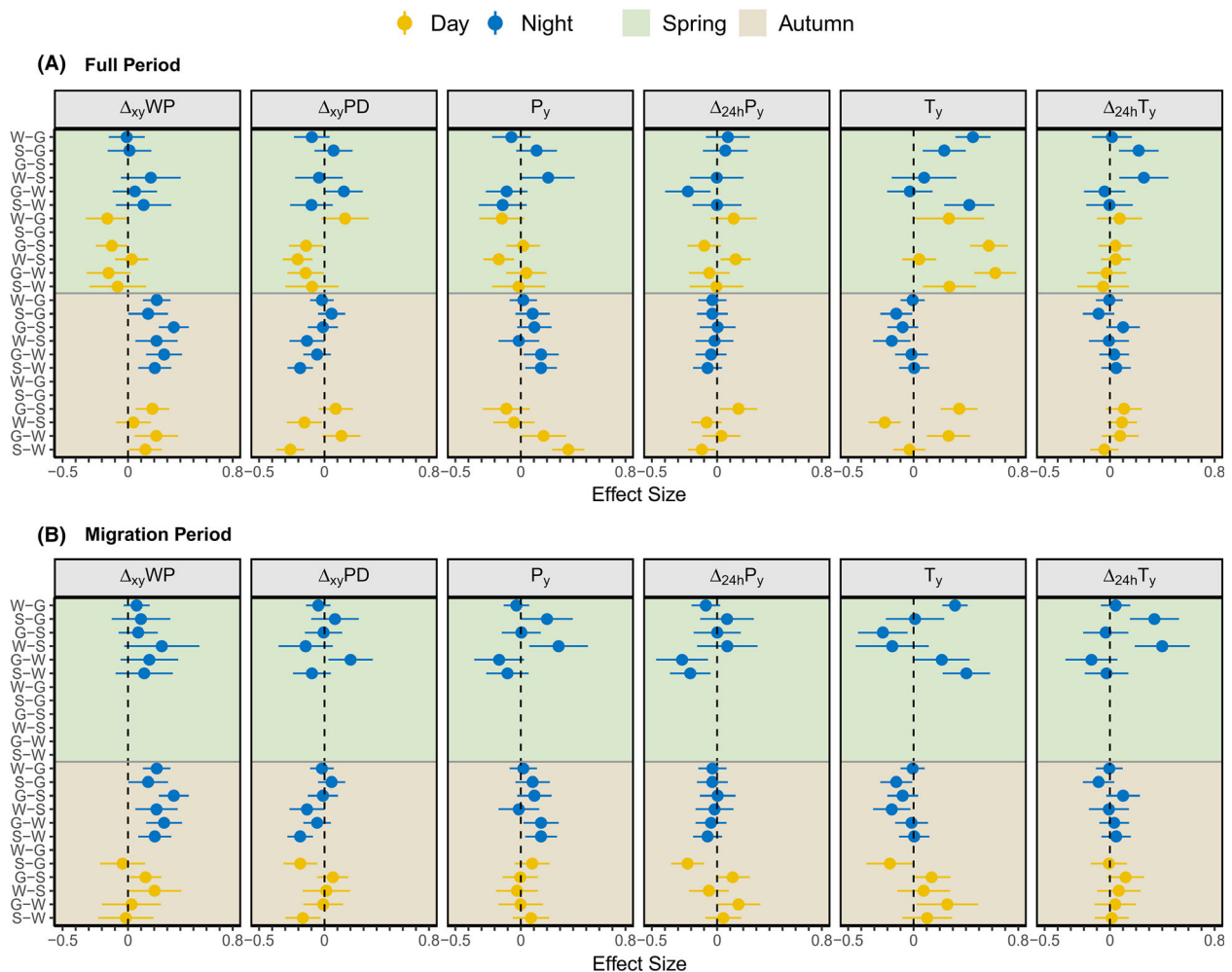


Figure 5. Effect sizes of the standardized atmospheric variables used as predictors in the BTR + Atmo models using (A) the full period, or (B) restricted to the main migration period. Parameter estimates (dots) with their 95% confidence intervals (lines) for the respective atmospheric variable (panels) are aligned vertically for each model. Labels indicate the site of the BTR data that was used as predictor (letter left of '-'), and the site at which BTRs were predicted (letter right of '-'): (W: Winterthur, S: Sempach, G: Geneva). Effects sizes for the different atmospheric variables are aligned horizontally across panels for each model. The upper half (greenish background) of the panel shows the results for spring models, the lower half (brownish background) for autumn models for diurnal (yellow symbols) and nocturnal migration (blue symbols). Atmospheric variables: $\Delta_{xy}WP$: wind profit differences between sites, $\Delta_{xy}PD$: precipitation duration differences between sites, P_y : barometric pressure at prediction site, $\Delta_{24h}P_y$: 24 h change in barometric pressure at prediction site, T_y : air temperature at prediction site, $\Delta_{24h}T_y$: 24 h change in air temperature at prediction site. Models for diurnal spring bird movements are not shown in (B), because the main migration period was missed. Only models without temporal autocorrelation are shown.

We assume that the higher consistency of bird movements in autumn compared to spring (Figs. 3 and 4) is related to the different topographical situation encountered by migrants approaching the Swiss lowlands with southwesterly directions in autumn and with northeasterly direction in spring. While in autumn the Alps guide the migratory flow across the Swiss lowlands (Bruderer and Jenni 1990; Bruderer and Liechti 1990; Bruderer 2017), the relatively low altitude of the Jura Mountains does not seem to guide the migratory movements in

spring as much as the Swiss Alps do in autumn. This would therefore lead to both a less consistent activity pattern and a lower concentration in flight directions for spring compared to autumn movements, which is what we observed. However, because we missed a substantial part of spring migration, our interpretation remains to be validated.

The effect of the between-sites differences of wind profit and precipitation was in line with our expectations that higher wind profits and less precipitation at the

prediction site compared to the explanatory site should lead to higher BTRs at the prediction site (Fig. 5B). The effect of pressure and temperature probably accounts for site-specific differences in the relationship between BTR and atmospheric conditions, that is, while all sites show an increase in BTR with favorable atmospheric conditions, the rate of increase can vary between sites. These differences in the effects of atmospheric conditions between sites may be related to the position of the site within the general migratory flow. For example, peaks during autumn migration occurred at very similar times at all sites, but were much higher in Geneva and Winterthur, which indicates that Sempach is somewhat at the edge of the migratory flow.

Our approach was different from previous studies in two aspects in particular. First, simultaneously operating ornithological radars at multiple sites during the spring and autumn migration season allowed us to compare quantitative migration patterns for both diurnal and nocturnal migration in both migration seasons. Although studies comparing quantitative migration patterns between locations are becoming more common thanks to the use of weather radar networks, these studies are restricted to nocturnal movements (e.g. Van Doren and Horton 2018; Weisshaupt et al. 2018; Nilsson et al. 2019), because an adequate method for extracting diurnal migration from these radars is still lacking (Dokter et al. 2019). In addition, studies predicting bird movement intensities have largely focused on autumn migration (e.g. Erni et al. 2002; Van Belle et al. 2007; Nilsson et al. 2019), with only a few studies on spring migration (e.g. Van Doren and Horton 2018). Second, we used a new modeling approach by using a site's observed BTR to predict another site's BTR (with and without atmospheric conditions), instead of a seasonal trend variable (e.g. Erni et al. 2002; Van Belle et al. 2007), or atmospheric conditions only (e.g. Van Doren and Horton 2018; Nilsson et al. 2019). While our modeling approach was neither suited nor intended to forecast BTRs (because observed BTRs were used as a predictor), or to study the influence of atmospheric conditions on BTRs (because the BTR predictor already contains much of the atmospheric information), it allowed us to assess the spatio-temporal consistency of the migratory flow both with and without accounting for site-specific atmospheric conditions. In addition, since we also operated the radars outside the main migration periods, we likely recorded other types of movements besides migratory movements, such as dispersal or foraging. These presumably mainly non-migratory movements, as indicated by their absence of directedness, varied greatly between sites but achieved intensities in the same order of magnitude as during peak migration.

Conclusion

The results in this study imply that bird migration intensities measured at a single location within the Swiss lowlands could very well predict the relative temporal pattern of nocturnal autumn migration at other locations, but not absolute intensities. Diurnal autumn migration could still be predicted fairly well, mainly when local atmospheric conditions were taken into account. Predictions for spring were much less reliable, probably because a major part of migration was missed. Unexpectedly, this study demonstrated that diurnal presumably non-migratory movements can achieve intensities close to peak diurnal migration intensities. These movements occurred within a limited area and could not be extrapolated to other sites, but may be relevant from a conservation perspective, e.g. for the protection of local colonies of aerial foragers.

Although nocturnal bird movement intensities in autumn were much higher than diurnal or spring bird movements, reliable predictions of diurnal bird movement intensities are also important, because diurnal migrants fly at lower altitudes (Bruderer et al. 2018) and are consequently at a higher risk for collisions with human structures, particularly during weather conditions with reduced visibility (Hüppop et al. 2006; Marques et al. 2014). Forecasting bird intensities for areas of increased collision risks can be improved by replacing simple extrapolations by models including bird behavior (e.g. Aurbach et al. 2018) or by implementing a network of constant monitoring sites. With respect to the complex terrain of a mountain area like Switzerland, a model approach alone will hardly provide a satisfactory result. Ideally, migration forecasts can be achieved with a dynamic model approach similar to those applied in weather forecasts, based on a network of year-round monitoring sites for near real-time calibration of the model, whereas including accurate information of atmospheric conditions can help to limit the number of measurement points.

Acknowledgments

We gratefully acknowledge the support of: Herbert Stark and Thomas Steuri (Swiss Ornithological Institute, SOI) for the radar logistics; Janine Aschwanden (SOI) for processing the bird radar data; Daniel Früh and Dominik Kleger from the University of Applied Sciences Winterthur (ZHAW) for operating their bird radar; Berberat for permission to use their land to place the radar device; MeteoSwiss for providing atmospheric data; Fränzi-Korner Nievergelt (SOI) for statistical advice; Lukas Jenni (SOI) for comments on this manuscript; all colleagues from the SOI, particularly from the bird migration

department, for fruitful discussions; two anonymous reviewers and Matthew Van Den Broeke for their comments and suggestions on an earlier draft of this manuscript.

Author Contributions

PT, FL, and BS conceived the study with suggestions from XS and LP. PT conducted the analyses and wrote the initial draft of the manuscript with substantial contributions from all authors.

Conflicts of Interest

None.

Data Availability

Echo, BTR and daily aggregated weather data used for this publication is available from Zenodo: <https://doi.org/10.5281/zenodo.3549719> (Tschanz et al. 2019). Precipitation data from the meteorological field stations operated by MeteoSwiss (www.meteoschweiz.admin.ch) is freely available for research purposes after registration to IDA-WEB (<https://gate.meteoswiss.ch/idaweb>). All other weather data was provided by MeteoSwiss from the COSMO-1 model for our study sites at cost, and not publicly available.

Funding Information

We thank the numerous donors of the SOI, who made this research possible.

Permits

Radar monitoring permitted by the Swiss Federal Office of Communications.

References

- Aurbach, A., B. Schmid, F. Liechti, N. Chokani, and R. Abhari. 2018. Complex behaviour in complex terrain - modelling bird migration in a high resolution wind field across mountainous terrain to simulate observed patterns. *J. Theor. Biol.* **454**, 126–138.
- Batschelet, E. 1981. *Circular statistics in biology*. Academic Press, London.
- Bauer, S., and B. J. Hoyer. 2014. Migratory animals couple biodiversity and ecosystem functioning worldwide. *Science* **344**, 1242552.
- Bauer, S., J. W. Chapman, D. R. Reynolds, J. A. Alves, A. M. Dokter, M. M. H. Menz, et al. 2017. From agricultural benefits to aviation safety: realizing the potential of continent-wide radar networks. *Bioscience* **67**, 912–918.
- Bauer, S., J. Shamoun-Baranes, C. Nilsson, A. Farnsworth, J. F. Kelly, D. R. Reynolds, et al. 2019. The grand challenges of migration ecology that radar aeroecology can help answer. *Ecography* **42**, 861–875.
- Bruderer, B. 1971. Radarbeobachtungen über den Frühlingszug im Schweizerischen Mittelland: Ein Beitrag zum Problem der Witterungsabhängigkeit des Vogelzugs. *Ornithol. Beob.* **68**, 89–158.
- Bruderer, B. 1997. The study of bird migration by radar part 2: major achievements. *Naturwissenschaften* **84**, 45–54.
- Bruderer, B. 1999. Three decades of tracking radar studies on bird migration in Europe and the Middle East. Pp 107–141 in Y. Leshem, Y. Mandelik, J. Shamoun-Baranes, ed. *Proceedings of the international seminar on birds and flight safety in the middle east*. Tel Aviv University, Tel Aviv.
- Bruderer, B. 2003. The radar window to bird migration. Pp. 347–358 in P. Berthold, E. Gwinner and E. Sonnenschein, eds. *Avian migration*. Springer, Berlin, Heidelberg.
- Bruderer, B. 2017. Vogelzug: eine schweizerische Perspektive. Ala, Schweizerische Gesellschaft für Vogelkunde und Vogelschutz, Sempach..
- Bruderer, B., and L. Jenni. 1990. Migration across the Alps. Pp. 60–77 in E. Gwinner, ed. *Bird migration*. Springer, Berlin, Heidelberg.
- Bruderer, B., and F. Liechti. 1990. Richtungsverhalten nachziehender Vögel in Süddeutschland und der Schweiz unter besonderer Berücksichtigung des Windeinflusses. *Ornithol. Beob.* **87**, 271–293.
- Bruderer, B., D. Peter, and F. Korner-Nievergelt. 2018. Vertical distribution of bird migration between the Baltic Sea and the Sahara. *J. Ornithol.* **159**, 315–336.
- Dokter, A. M., P. Desmet, J. H. Spaaks, S. van Hoey, L. Veen, L. Verlinden, et al. 2019. bioRad: biological analysis and visualization of weather radar data. *Ecography* **42**, 852–860.
- Erni, B., F. Liechti, L. G. Underhill, and B. Bruderer. 2002. Wind and rain govern the intensity of nocturnal bird migration in central Europe - a log-linear regression analysis. *Ardea* **90**, 155–166.
- Faraway, J. J. 2006. *Extending the linear model with R: generalized linear, mixed effects and nonparametric regression models*. Chapman & Hall/CRC, Boca Raton, FL.
- GADM. 2018. GADM database of global administrative areas, version 3.6. <https://gadm.org/>
- Hüppop, O., J. Dierschke, K.-M. Exo, E. Fredrich, and R. Hill. 2006. Bird migration studies and potential collision risk with offshore wind turbines. *The Ibis* **148**, 90–109.
- Hüppop, O., M. Ciach, R. Diehl, D. R. Reynolds, P. M. Stepanian, and M. H. M. Menz. 2019. Perspectives and challenges for the use of radar in biological conservation. *Ecography* **42**, 912–930.

- Jarvis, A., H. I. Reuter, A. Nelson, and E. Guevara. 2008. Hole-filled seamless SRTM data version 4. <http://srtm.csi.cgiar.org>
- Kemp, M. U., J. Shamoun-Baranes, E. E. van Loon, J. D. McLaren, A. M. Dokter, and W. Bouten. 2012. Quantifying flow-assistance and implications for movement research. *J. Theor. Biol.* **308**, 56–67.
- Kirby, J. S., A. J. Stattersfield, S. H. M. Butchart, M. I. Evans, R. F. A. Grimmett, V. R. Jones, et al. 2008. Key conservation issues for migratory land- and waterbird species on the world's major flyways. *Bird Conserv. Int.* **18**, S49–S73.
- Liechti, F., D. Peter, R. Lardelli, and B. Bruderer. 1996. The Alps, an obstacle for nocturnal broad front migration – a survey based on moon-watching. *J. Ornithol.* **137**, 337–356.
- Liechti, F., J. Guélat, and S. Komenda-Zehnder. 2013. Modelling the spatial concentrations of bird migration to assess conflicts with wind turbines. *Biol. Cons.* **162**, 24–32.
- Liechti, F., J. Aschwanden, J. Blew, M. Boos, R. Brabant, A. M. Dokter, et al. 2019. Cross-calibration of different radar systems for monitoring nocturnal bird migration across Europe and the Near East. *Ecography* **42**, 887–898.
- Loss, S. R., T. Will, S. S. Loss, and P. P. Marra. 2014. Bird–building collisions in the United States: estimates of annual mortality and species vulnerability. *Condor* **116**, 8–23.
- Lowery, G. H. 1951. *A quantitative study of the nocturnal migration of birds*. University of Kansas, Lawrence.
- Marques, A. T., H. Batalha, S. Rodrigues, H. Costa, M. J. R. Pereira, C. Fonseca, et al. 2014. Understanding bird collisions at wind farms: an updated review on the causes and possible mitigation strategies. *Biol. Cons.* **179**, 40–52.
- Metz, I. C., J. Ellerbroek, T. Mühlhausen, D. Kügler, and J. M. Hoekstra. 2017. Simulating the risk of bird strikes. *Page Proceedings of the Seventh SESAR Innovation Days, 28th – 30th November 2017*. Belgrade, Serbia.
- Newton, I. 2008. *The migration ecology of birds*. Elsevier Academic Press, Amsterdam.
- Nilsson, C., A. M. Dokter, B. Schmid, M. Scacco, L. Verlinden, J. Bäckman, et al. 2018. Field validation of radar systems for monitoring bird migration. *J. Appl. Ecol.* **55**, 2552–2564.
- Nilsson, C., A. M. Dokter, L. Verlinden, J. Shamoun-Baranes, B. Schmid, P. Desmet, et al. 2019. Revealing patterns of nocturnal migration using the European weather radar network. *Ecography* **42**, 876–886.
- Nussbaumer, R., L. Benoit, G. Mariethoz, F. Liechti, S. Bauer, and B. Schmid. 2019. A geostatistical approach to estimate high resolution nocturnal bird migration densities from a weather radar network. *Remote Sens.* **11**, 2233.
- R Core Team. 2019. *R: a language and environment for statistical computing*. R Foundation for Statistical Computing, Vienne, Austria.
- Richardson, W. J. 1990. Timing of bird migration in relation to weather: updated review. Pp. 78–101 in E. Gwinner, ed. *Bird migration*. Springer, Berlin, Heidelberg.
- Sanderson, F. J., P. F. Donald, D. J. Pain, I. J. Burfield, and F. P. J. van Bommel. 2006. Long-term population declines in Afro-Palaearctic migrant birds. *Biol. Cons.* **131**, 93–105.
- Schmid, B., S. Zaugg, S. C. Votier, J. W. Chapman, M. Boos, and F. Liechti. 2019. Size matters in quantitative radar monitoring of animal migration: estimating monitored volume from wingbeat frequency. *Ecography* **42**, 931–941.
- Shamoun-Baranes, J., W. Bouten, L. Buurma, R. DeFusco, A. Dekker, H. Sierdsema, et al. 2008. Avian information systems: developing web-based bird avoidance models. *Ecol. Soc.* **13**, 38.
- Shamoun-Baranes, J., H. van Gasteren, and V. Ross-Smith. 2017. Sharing the aerosphere: conflicts and potential solutions. Pp. 465–497 in P. B. Chilson, W. F. Frick, J. F. Kelly and F. Liechti, eds. *Aeroecology*. Springer International Publishing, Cham.
- Sheather, S. 2009. *A modern approach to regression with R*. Springer, New York, New York, NY.
- Strandberg, R., and T. Alerstam. 2007. The strategy of fly-and-forage migration, illustrated for the osprey (*Pandion haliaetus*). *Behav. Ecol. Sociobiol.* **61**, 1865–1875.
- Tschanz, P., L. Pellissier, X. Shi, F. Liechti, and B. Schmid. 2019. Consistency of spatio-temporal patterns of avian migration across the Swiss lowlands [Data Set]. <https://doi.org/10.5281/zenodo.3549719>
- Van Belle, J., J. Shamoun-Baranes, E. Van Loon, and W. Bouten. 2007. An operational model predicting autumn bird migration intensities for flight safety. *J. Appl. Ecol.* **44**, 864–874.
- Van Doren, B. M., and K. G. Horton. 2018. A continental system for forecasting bird migration. *Science* **361**, 1115–1118.
- Van Doren, B. M., K. G. Horton, A. M. Dokter, H. Klinck, S. B. Elbin, and A. Farnsworth. 2017. High-intensity urban light installation dramatically alters nocturnal bird migration. *Proc. Natl Acad. Sci.* **114**, 11175–11180.
- Vickery, J. A., S. R. Ewing, K. W. Smith, D. J. Pain, F. Bairlein, J. Škorpirová, et al. 2014. The decline of Afro-Palaearctic migrants and an assessment of potential causes. *The Ibis* **156**, 1–22.
- Weisshaupt, N., A. M. Dokter, J. Arizaga, and M. Maruri. 2018. Effects of a sea barrier on large-scale migration patterns studied by a network of weather radars. *Bird Study* **65**, 232–240.
- Weitnauer, E. 1980. *Mein Vogel: aus dem Leben des Mauerseglers Apus apus*. Basellandschaftlicher Vogelschutzverband, Tenniken.
- Winkler, R. 1999. *Avifauna der Schweiz*. Zweite, neu bearb. Aufl. Ala, Schweizerische Gesellschaft für Vogelkunde und Vogelschutz, Möhlin.
- Zaugg, S., G. Saporta, E. E. Van Loon, H. Schmaljohann, and F. Liechti. 2008. Automatic identification of bird targets with radar via patterns produced by wing flapping. *J. R. Soc. Interface* **5**, 1041–1053.

Zuur, A., E. N. Ieno, and G. M. Smith. 2007. *Analyzing ecological data*. Springer-Verlag, New York.

Supporting Information

Additional supporting information may be found online in the Supporting Information section at the end of the article.

Figure S1. Between-site comparison of (A) wind profit, (B) precipitation duration, (C) air pressure, and (D) air temperature.

Figure S2. Scatterplots (upper triangle) and Spearman's rank correlation coefficient (lower triangle) of observed

bird traffic rates (BTRs) between the three sites Geneva (GEN), Sempach (SEM), and Winterthur (WNT) for (A) diurnal spring, (B) nocturnal spring, (C) diurnal autumn, and (D) nocturnal autumn bird movements for the full period.

Figure S3. Same as Fig. S2, but with data restricted to the main migration period. No plot is shown in (A), because the main diurnal spring period was missed.

Table S1. Description of explanatory variables used in the generalized linear models.

Table S2. Mean, standard deviation (SD), minimum (Min) and maximum (Max) Spearman's rank correlation coefficient ρ per season, time of day (ToD), and model type.